The 19th Pacific Basin Nuclear Conference (PBNC 2014)
Hyatt Regency Hotel, Vancouver, British Columbia, Canada, August 24-28, 2014.

PBNC2014-211

FUEL CRACKING IN RELATION TO FUEL OXIDATION IN SUPPORT OF AN OUT-REACTOR INSTRUMENTED DEFECTED FUEL EXPERIMENT

A. Quastel[1], C. Thiriet[1], B. Lewis[2], E. Corcoran[3]
[1]Atomic Energy of Canada Limited, Chalk River, Ontario, Canada
[2]University of Ontario Institute of Technology, Oshawa, Ontario, Canada
[3]Royal Military College of Canada, Kingston, Ontario, Canada
quastela@aecl.ca, thirietc@aecl.ca, brent.lewis@uoit.ca, emily.corcoran@rmc.ca

Abstract

An experimental program funded by the CANDU® Owners Group (COG) is studying an out-reactor instrumented defected fuel experiment in Stern Laboratories (Hamilton, Ontario) with guidance from Atomic Energy of Canada Limited (AECL). The objective of this test is to provide experimental data for validation of a mechanistic fuel oxidation model. In this experiment a defected fuel element with UO_2 pellets will be internally heated with an electrical heater element, causing the fuel to crack. By defecting the sheath in-situ the fuel will be exposed to light water coolant near normal reactor operating conditions (pressure 10 MPa and temperature 265-310°C) causing fuel oxidation, especially near the hotter regions of the fuel in the cracks. The fuel thermal conductivity will change, resulting in a change in the temperature distribution of the fuel element. This paper provides 2D r-θ plane strain solid mechanics models to simulate fuel thermal expansion, where conditions for fuel crack propagation are investigated with the thermal J integral to predict fuel crack stress intensity factors. Finally since fuel crack geometry can affect fuel oxidation this paper shows that the solid mechanics model with pre-set radial cracks can be coupled to a 2D r-θ fuel oxidation model.

Introduction

The fuel element sheath (clad) in nuclear fuel prevents the release of fission products into the coolant and protects the fuel from being oxidized. A small breach can occur in the sheathing during normal reactor operation as a result of debris fretting, pellet-cladding interaction or manufacturing defects. Such sheath breaches allow coolant to make direct contact with the fuel, leading to fuel oxidation [1]. As the fuel is oxidized, the fuel thermal conductivity will be degraded, resulting in higher fuel temperatures [2]. Moreover, in hyper-stoichiometric fuel, the melting temperature will be reduced, possibly leading to centreline fuel melting in high-powered elements, particularly during accident conditions [3]. Fission product release will also be enhanced by a greater mobility in the hyper-stoichiometric fuel [1]. A mechanistic fuel oxidation model for defective fuel was developed at the Royal Military College of Canada (RMC) to predict UO_2 fuel oxidation under normal operating conditions [4].

In the current work, the fuel oxidation model has been extended for the design of an out-reactor fuel oxidation test. This test will be used to validate the fuel oxidation model [4]. An out-reactor instrumented defected fuel experiment funded by CANDU® Owners Group (COG), managed by

AECL-CRL (Atomic Energy of Canada Limited - Chalk River Laboratories), is being conducted by Stern Laboratories. Figure 1 shows the axial and radial cross-section of the instrumented defected fuel element simulator, showing fuel pellets, electrical heating element and thermocouples (TC) in two axial planes, A and B. The motivation for the proposed experiment is that fuel oxidation has never been investigated experimentally at both coolant pressure (~10 MPa) and reactor temperatures while simultaneously measuring in-situ fuel temperatures (and hence fuel thermal conductivity). The proposed experiment incorporates controlled parameters such as an in-situ initiated sheath defect of a specific size, heating duration and heating power.

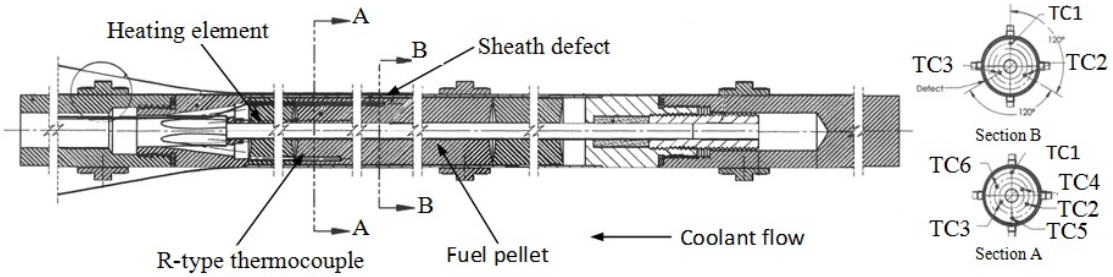

Figure 1 Test section with thermocouple locations in two axial planes (Section A and Section B) of the out-reactor instrumented defected fuel experiment at Stern Laboratories.

In an earlier paper [5], two independent 2D r-θ models were presented - one modeled fuel oxidation with preset radial fuel cracks that included heat transfer, solid state diffusion and gas diffusion. The second model included thermally expanded radial fuel cracks where conditions for fuel crack propagation using solid mechanics physics were assessed. It was shown [5] that fuel oxidation is sensitive to the fuel radial crack and the fuel-to-sheath gap widths. Since the fuel thermal conductivity is dependent on the extent of fuel oxidation and since thermal conductivity determines the temperature distribution in a material, then fuel oxidation can affect the thermal expansion of the solid fuel. This in turn can affect the number and width of the radial fuel cracks in the fuel, and hence the extent of fuel oxidation. In the out-reactor fuel oxidation experiment, with the applied post-defect residence times (days) and heating power, the degree of fuel oxidation should be enough to slightly affect the thermal conductivity of the fuel so that it can be measured, but not enough to substantially change the thermal expansion of the fuel. Nevertheless, coupling the fuel oxidation and fuel pellet solid mechanics models may be useful to accurately determine the extent of fuel oxidation and the possible onset of fuel melting in high powered fuel elements for in-reactor defective fuel, due to possible extended post-defect residence times (weeks and months) [4] and higher heating powers.

In the current paper two models are presented. In the model, the stress distribution in the heated out-reactor fuel element is modeled with solid mechanics as in [5], with the additional consideration of plasticity of the inner fuel. This has an effect on the computed stress intensity factor of a fuel crack tip that is developing from a fuel pellet surface flaw, which is investigated as a steady state finite element analysis (FEA) problem. Furthermore, for assessing the stress intensity factor at the crack tip, the J integral was computed considering a thermal stress field to ensure J integral contour path independence. A second model then couples the solid mechanics model, which includes thermally expanded fuel cracks, with the fuel oxidation model [4,5] using the Arbitrary Lagrangian Eulerian

(ALE) deformed mesh method. Both models are configured in 2D r-θ dimensions. COMSOL Multiphysics® Version 4.3b FEA software package was used for this purpose.

1. Theory

Section 1.1 covers the theory for the solid mechanics model considering thermal expansion accompanied with a J integral computation in a thermal stress field. Section 1.2 describes the coupling of the solid mechanics model containing thermally expanded fuel cracks with the fuel oxidation model.

1.1 Fuel thermal expansion and fuel cracking conditions

The *solid mechanics* plane strain model considered thermal expansion of the fuel pellet and Zircaloy sheathing. To achieve this, the stress and strain fields in the model were solved by applying the general stress-strain relation expressed in the following equation [6,7]:

$$\sigma_{ij} = C_{ijkl}\left(\varepsilon_{kl} - \alpha\left(T - T_{ref}\right)\delta_{kl} - \varepsilon_{p}\right) \quad (1)$$

where σ_{ij} is the stress tensor, C_{ijkl} is the fourth order elasticity or elastic stiffness tensor, ε_{kl} is the total strain tensor, α is the thermal expansion coefficient, T is the temperature in K, T_{ref} is the reference temperature (set to ambient temperature), ε_p is the plastic strain tensor and δ_{kl} is the Kroneker delta [6,7]. The following table provides equations for the mechanical properties of the fuel element materials used in the plane strain model:

Table 1 Mechanical properties of stoichiometric UO_2 and Zircaloy.

Term	Description	Expression	Ref.
E_{UO2}	Young's modulus of UO_2	$2.334\text{x}10^{11}\left(1-2.752\left(1-D\right)\right)\cdot\left(1-1.0915\text{x}10^{-4}T\right)$ [Pa] for $300\text{ K} < T < 3113\text{ K}$ where D is the fraction from theoretical density	[8]
ν_{UO2}	Poisson's ratio of UO_2	$\nu_{UO2} = 1.32\left(1-0.26P\right)-1$ where P is fuel porosity	[9]
α_{UO2}	UO_2 coefficient of thermal expansion	$9.828x10^{-6} - 6.390x10^{-10}T + 1.330x10^{-12}T^2 - 1.757x10^{-17}T^3$ for $273\text{K} \le T \le 923\text{K}$ $1.1833x10^{-5} - 5.013x10^{-9} + 3.756x10^{-12}T^2 - 6.125x10^{-17}T^3$ for $923\text{K} \le T \le 3120\text{K}$	[10]
$E_{Zircaloy}$	Young's modulus of Zircaloy	$\left(1.088\times10^{11} - 5.475\times10^{7}T + K_{1\_Zirc} + K_{2\_Zirc}\right)/K_{3\_Zirc}$ for $300\text{ K} < T < 1083\text{ K}$ where coefficients K are given in Ref.	[8]
$\nu_{Zircaloy}$	Poisson's ratio of	0.37	[11]
$\alpha_{Zircaloy}$	Zircaloy coefficient of thermal expansion	$\frac{\varepsilon_{11}}{\left(T - T_{ref}\right)}$ for $300\text{ K} < T < 1083\text{ K}$ where $\varepsilon_{11} = 4.95x10^{-6}T - 1.485x10^{-3}$s for $300\text{ K} < T < 1083\text{ K}$	[8]

Notes: A value of 0.0328 was given for P, the coefficients K are additional equations given in [8] and T_{ref} is the reference temperature 298 K.

In addition to elastic modelling of the fuel, the Zircaloy sheath was allowed to plastically deform when in contact with the fuel at an initial yield stress of a 150 MPa [12] with an isotropic tangent modulus (after yielding) set to 1/10 the Young's modulus [13]. For the inner plastic UO_2 core (see also discussion is Section 1.2) the initial yield stress was set to 147 MPa and the isotropic tangent modulus was set to 588.6 MPa [14]. It should be mentioned that the UO_2 fracture stress occurs between 80-150 MPa, due to elevated stress intensities at internal and external fuel pores and flaws [8,9,15], so fuel plastic yielding will probably coincide with fuel cracking. Nevertheless both phenomena lead to stress relaxation in the fuel at elevated temperatures. The following figure graphically presents these values for: (a) Zircaloy-4, and (b) UO_2 at normal in-reactor operating temperatures:

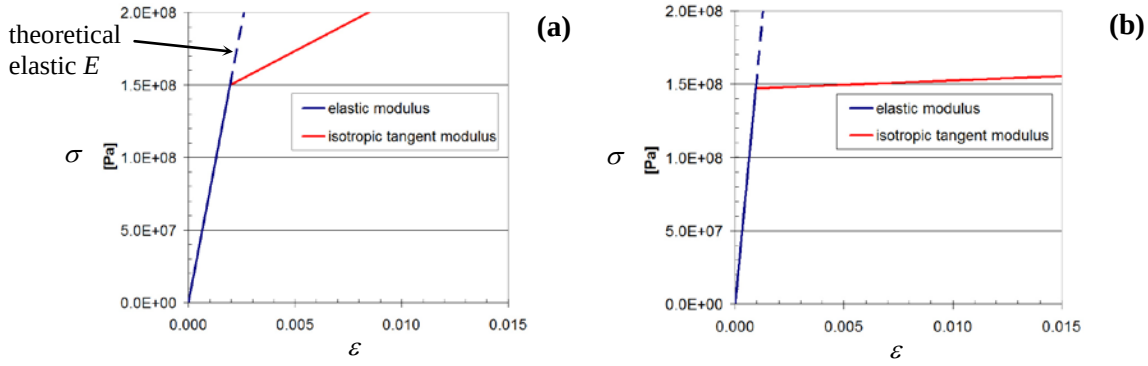

Figure 2 Stress-strain curves with elastic and plastic hardening Young's modulus for: (a) Zircaloy-4 at 580 K and (b) for stoichiometric UO_2 at 1473 K.

where the solid blue line (steeper slopes) represents the elastic modulus and the red line (less steep slopes) represents the isotropic tangent modulus after yielding where material hardening also occurs.

Frictionless contact modelling between the fuel pellet and the sheath was achieved using a penalty method [16]. Although the contribution of fuel pellet and fuel sheath mechanical contact is minimal in respect to affecting the resulting crack geometry and the number of fuel cracks created (since the fuel stiffness is much greater than sheath stiffness) it is included for the sake of investigating mechanical contact with heat transfer across the sheath.

The conditions for crack propagation were assessed by computing the *J* integral. The *J* integral provides a measure of the intensity of stresses and strains at the crack tip and has the units of J m^{-2} (energy per fracture surface area). The *J* integral is given by [5,17,18]:

$$J = \int_{\Gamma} \left(w dy - T_i \frac{\partial u_i}{\partial x} ds \right) \qquad (2)$$

The above described *J* integral computation is a path independent line integral (*i.e.*, arbitrary line integration paths around the crack tip yield the same *J* value) and is applicable for bodies in isothermal, steady state temperature distributions. Yet when a temperature gradient exists (parallel to the crack growth direction), inducing thermal stresses in the body (due to thermal expansion), the computed *J* integral can become path dependent, which is undesirable. To overcome this problem Wilson and Yu [19] modified the conventional *J* integral to include an area integral that compensates for the

temperature gradient in thermal stress problems. The modified equation is referred to here as the *J** integral and it describes the energy release rate to crack extension, which is given by Aoki *et al.* [20] as:

$$J^* = \int_{\Gamma} w_e dy - \int_{\Gamma} T_i \frac{\partial u_i}{\partial x} ds + \alpha \iint_{A} \sigma_{kk} \frac{\partial \theta}{\partial x} dA \tag{3}$$

where w_e is the elastic strain energy density, T_i is the traction vector, u_i the displacement vector components, ds is the length increment along the integration contour, σ_{kk} is the principle stress tensor, α is the thermal expansion coefficient (considered here as a constant), θ is the temperature increment from the reference temperature and A is the area of the J integral contour.

For assessing the stress intensity factor K_I around a developing crack tip under mode I loading (purely tensile stress) and steady state conditions, Eq. (4) is evaluated [21]:

$$K_I = \sqrt{J \frac{E}{(1-\nu^2)}} \tag{4}$$

where J is the J (or J^*)-integral, E is the Young's modulus and ν is the Poisson ratio applied here to UO_2 fuel. Favorable conditions for crack propagation can then be determined by comparing computed K_I values at crack tips to analytical or measured values of K_{Ic} (*i.e.*, when K_I values exceeds the fracture toughness K_{Ic}) in this case the fracture toughness of sintered UO_2 fuel [5,22].

Lastly, the width of the cracks can affect the extent of fuel oxidation [5], and thus it is required that the gas domain in the fuel cracks match the deforming solid fuel domain boundaries. To avoid regenerating a new mesh in the fuel cracks at each new configuration of the solid fuel boundaries, the software moves the mesh nodes so they conform with the moved boundaries (using ALE).

1.2 Fuel oxidation model

The mechanistic fuel oxidation model considers heat conduction, gas transport in fuel cracks and gaps and solid state oxygen diffusion in the fuel. Figure 3 illustrates the radial cross-section of the out-reactor fuel oxidation fuel element simulator, showing the heater element, the fuel, the radial fuel cracks and the fuel sheath with an intentional sheath breach.

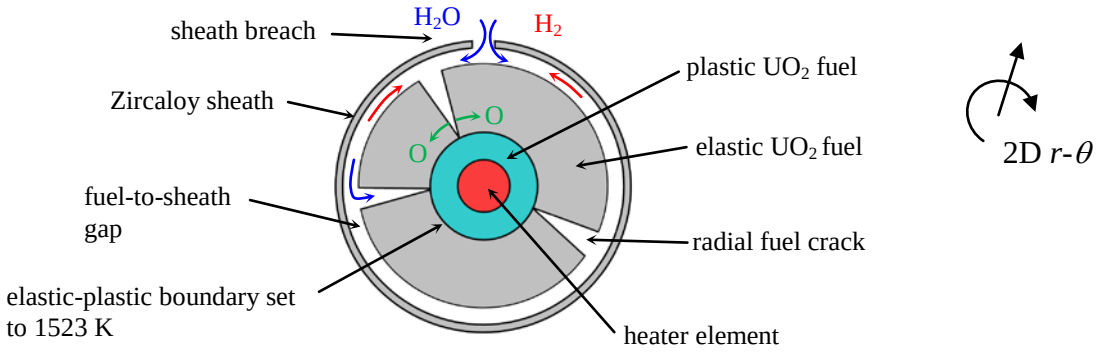

Figure 3 A 2D representation of the out-reactor fuel element cross-section pertaining to the fuel oxidation model (not to scale).

Cracks created in the fuel pellets are a result of fuel thermal expansion [15]. Below the elastic-plastic boundary, cracks initially appear, but later self-heal [23]. The temperature at which this transition occurs was selected in the models as 1523 K (as in reality it occurs over a temperature range between 1473-1673 K [9,15]). When the sheath defect is initiated, the coolant (in this case H_2O seen as blue arrows in Figure 3) can contact and oxidize the fuel. Hydrogen generated in the reaction (seen as red in Figure 3) diffuses to the sheath breach and out to the coolant. Hydrogen can also hydride the Zircaloy sheath. Elevated oxidation occurs though at the hotter regions of the fuel via the fuel cracks. The generalized mass balance equation for oxygen transport in the fuel is given by the following equation:

$$c_u \frac{\partial x}{\partial t} = c_u \nabla \cdot \left(D \left(\nabla x + x \frac{Q}{RT^2} \nabla T \right) \right) + R_f^{react} \tag{5}$$

where D is the diffusion coefficient for oxygen interstitials in the solid matrix, x (also written as Xdev) is the oxygen deviation from stoichiometry in the UO_2 fuel (written as UO_{2+x}), c_u is the molar density of uranium in mol m^{-3}, R is the universal gas constant in atm m^3 mol^{-1} K^{-1}, Q is the molar effective heat transport in J mol^{-1}, T is temperature in K and R_f^{react} is the reaction rate source term for either fuel oxidation or reduction in moles $0.5O_2$ or H_2 m^{-2} s^{-1} [4,5] production.

The mass balance for the hydrogen mole concentration (qc_g) in the fuel cracks and fuel-to-sheath gap is given by:

$$c_g \frac{dq}{dt} = \nabla \cdot \left(c_g D_g \nabla q \right) + R_f^{react} \tag{6}$$

where q is the hydrogen mole fraction, c_g is the total molar concentration of gas in mol m^{-3}, and $c_g D_g$ is the gas diffusivity quantity in mol m^{-1} s^{-1} [4,5]. Eq. (6) is applicable only in the elastic domain above the elastic-plastic boundary in the fuel cracks and pellet-pellet gap (Figure 3). The interaction of gas in the fuel cracks and the cracked fuel surfaces is a heterogeneous (gas and solid) chemical reaction. In the current model, the oxygen diffusion equation, Eq. (5), and the gas diffusion equation, Eq. (6), occur in separate domains where the source term, R_f^{react}, is equal to zero. Nevertheless these terms are not equal to zero at common fuel-to-gas boundaries (in the cracks). Here Eq. (5) and Eq. (6) are coupled together at common fuel-to-gas domain surfaces (in the fuel cracks), where the source terms act as inward flux terms [5].

Lastly, the temperature profile in the fuel element was obtained from a solution of the heat conduction equation:

$$\rho_s C_p \frac{\partial T}{\partial t} = \nabla \cdot \left(k \nabla T \right) + Q_{heat} \tag{7}$$

where ρ_s is the fuel density, C_p is the specific heat of the fuel, k is the thermal conductivity of the fuel and Q_{heat} is the volumetric heat source term. In the current 2D r-θ model, the Q_{heat} term is the ohmic heating generated in an iridium central heater element and in the Zircaloy sheath. In the model, C_p and k are functions of T and x, while R_f^{react} is a function of T, x, and q, making this model highly non-linear.

As manufactured, there is a small radial gap between the fuel pellets and the inner surface of the sheath. During operation, this gap eventually closes due to coolant pressure on the sheath and thermal expansion of the pellets. In regions with fuel-to-sheath contact, heat is transported by conduction, while heat is conducted through the gas film that fills the portion of the interface where there is no physical contact between the fuel and the sheath [1,9]. The effective thermal conductivity value in the fuel-to-sheath gap is given by [24,25]:

$$k_{gap\_effective} = \frac{h_{solid} + h_{gas}}{h_{gas}} k_{gas} \quad (8)$$

where h_{solid} is the solid heat transfer coefficient, h_{gas} is the gas heat transfer coefficient and k_{gas} is the thermal conductivity of the gas in the gap at the gap mean temperature. Preliminary prototype tests of the out-reactor fuel oxidation test indicate that the fuel-to-sheath gap is open (*i.e.*, a few μm wide) due to the short conditioning period in the test. Hence for an open fuel-to-sheath gap, the thermal conductivity of the gap was modelled using only the thermal conductivity of the gas in the gap, k_{gas}, *i.e.*, steam for the defected fuel element.

For more details on the fuel oxidation model refer to [4,5].

2. Model results

2.1 Fuel cracking and solid mechanics analysis

The mesh used in the plane strain model is illustrated in Figure 4. The stress intensity around a crack tip developing from a surface flaw (located in the green circle at the 9 o'clock position in the figure) with one pre-set, full length, radial crack initially 3 μm wide, at the 3 o'clock position, was investigated. The remaining radial cracks seen at the 11, 12, 1 and 6 o'clock positions were disabled and were defined as solid UO_2 fuel in order to analyse this higher stress case (in Section 2.2 of this paper and in [5] these latter cracks were allowed to thermally expand open to investigate a lower stress case). The mesh was entirely quadrilateral elements except for the central heater which was meshed with triangular elements since its domain was computed only for a heat transfer result (*i.e.*, no solid mechanics requiring quadrilateral elements). Quadratic shape functions were applied for all physics. Figure 5 shows close up views of the fuel pellet surface flaw with: (a) 0.25 mm sided square *J* integral contour, and (b) 0.5 mm diameter circle *J* integral contour. The purpose here was to show contour shape and size independence when computing the *J* integral.

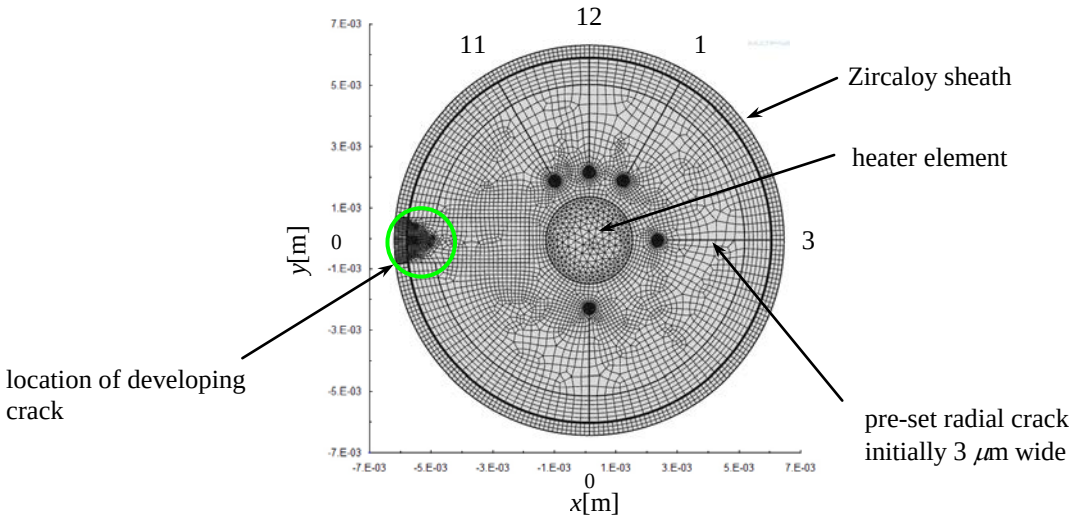

Figure 4 Finite element analysis quadrilateral meshed with crack positions.

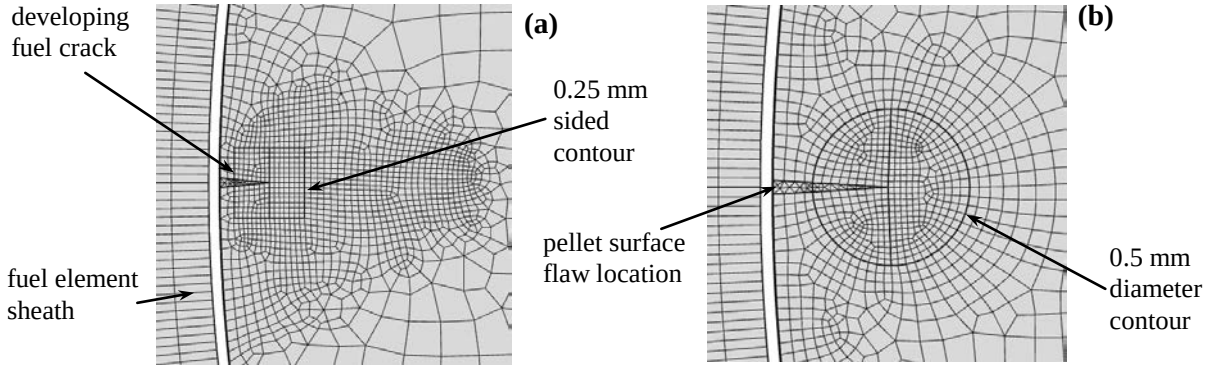

Figure 5 Applied quadrilateral meshes and the *J* integral contour that is: (a) 0.25 mm sided square contour, and (b) 0.5 mm diameter circle contour.

Figure 6 provides the von Mises stress distribution model results in the heated element for two cases: (i) when UO_2 core plasticity is considered by applying the information in Figure 2 (b), and (ii) when UO_2 plasticity is not considered, where only elastic behaviour is considered. Figure 6 (a) shows a blue inner ring (low stress) that indicates the fuel plastic core, whereas in Figure 6 (b) there is no stress relaxation and stress is at a maximum at both the inner pellet annulus and at the crack tips. The von Mises stress in the model that considers also a plastic UO_2 core is less than the model that considers only elastic UO_2.

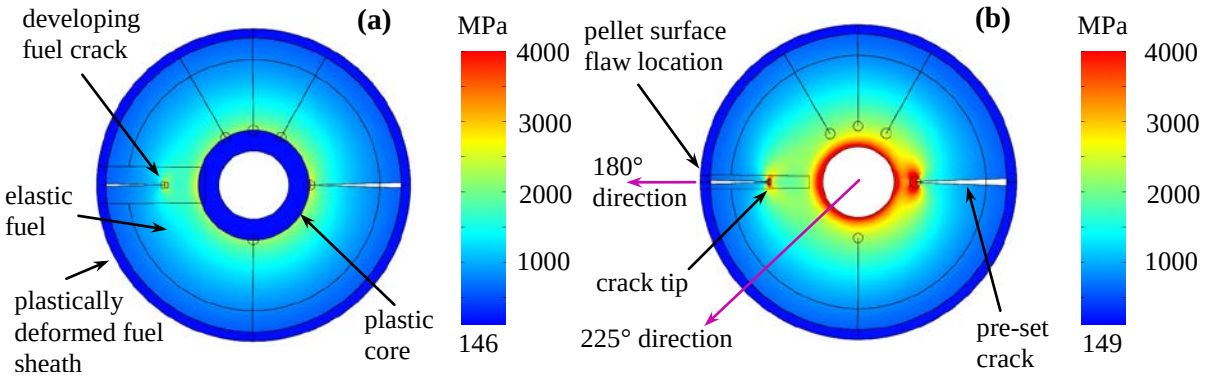

Figure 6 von Mises stress distribution in: (a) a model that considers fuel core plasticity (dark blue inner area), and (b) in a model that considers only elastic fuel [5].

Figure 7 provides the azimuthal and radial stresses vs. the radial position in the fuel element, for the two cases shown in Figure 6, at two plotted angles through the fuel element: at (i) 180 degrees, and (ii) at 225 degrees. For the case with a plastic core (Figure 7 (a)) the azimuthal and radial stress, in the plastic region, are slightly compressive <220 MPa. Whereas in Figure 7 (b), which considers only an elastic core, the maximum azimuthal stress is >4 GPa compressive and the maximum radial stress is ≈900 MPa compressive, in the same region. Since the azimuthal tensile stress is of interest when considering mode *I* cracking in the fuel pellet it is worth pointing out in Figure 7 (a) that the azimuthal stress only becomes tensile when at the radial position of 4.5 mm from the fuel element centre (or about 1.5 mm from the pellet surface), when looking at the 225 degree plot (blue curve). On the other hand when only elastic behaviour is considered, Figure 7 (b), the azimuthal and radial stresses in both radial plots (blue and light blue curves) become tensile when at the radial position of 3 mm from the fuel element centre (or about 3 mm from the pellet surface). Hence it seems that when a plastic fuel core is considered the overall stress in the fuel will be reduced leading to possibly less radial cracks from forming in the out-reactor fuel pellets with an inner annulus, assuming that a fuel plastic core forms before fuel cracking commences.

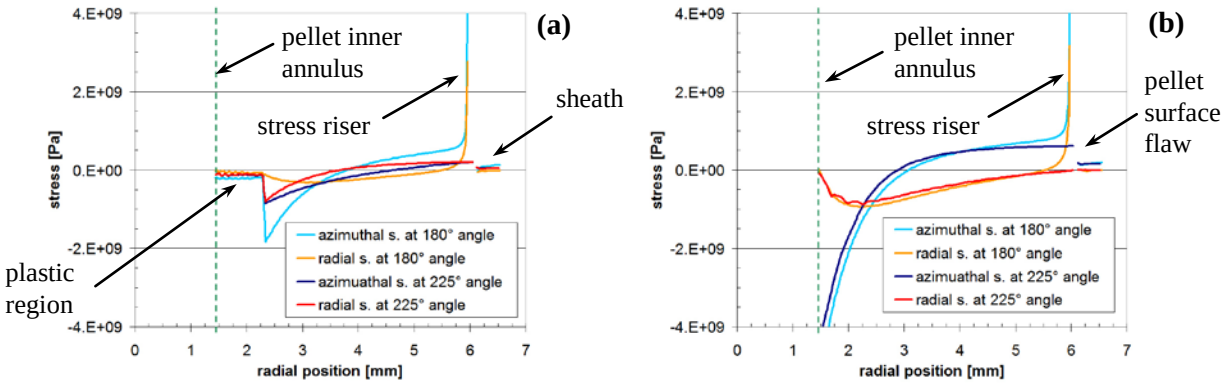

Figure 7 Radial and azimuthal stresses vs. radial position for: (a) a model that considers fuel core plasticity, and (b) a model that considers only elastic fuel [5].

Favorable conditions for crack propagation were investigated in the pellet with one full length pre-set radial crack and one surface flaw developing into a crack by computing Eq. (4) for discrete crack length

increases. These values can then be compared to UO_2 fracture toughness values [5,22]. As can be seen in Figure 8 the plane strain plastic core stress intensity values, K_I, (green line and red diamonds) are over an order of magnitude greater than analytical and measured fracture toughness values (yellow triangle and green square), indicating favorable conditions for additional cracks to form (greater than the two modeled cracks in Figure 6). But these K_I values are also lower that the elastic plane strain model K_I values (blue line), as expected, due to the stress relaxation in the plastic core.

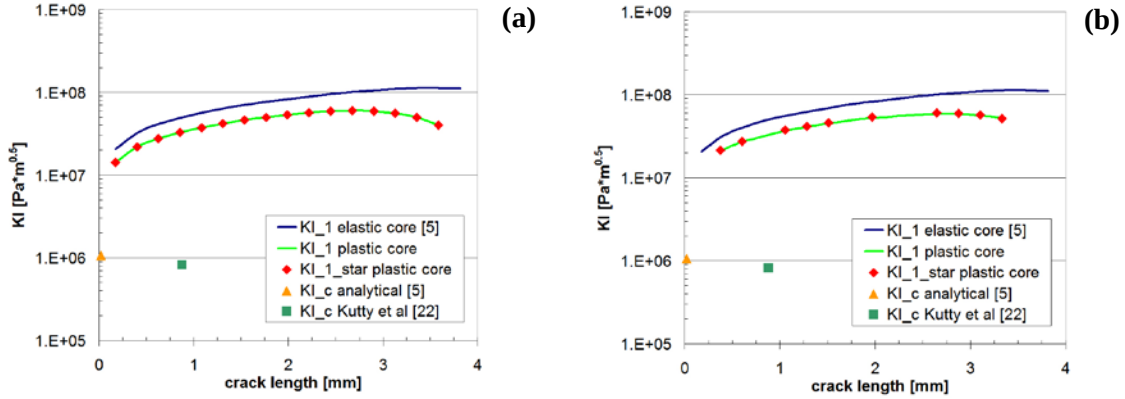

Figure 8 Stress intensity factors vs. crack length in a model that considers fuel core plasticity computed with: (a) 0.25 mm sided square and (b) 0.5 mm diameter circle integration contours.

From Figure 8 (a) and (b) there is almost no difference between the K_I values computed using the J integral (green line, Eq. (2)) and using J^* integral (red diamonds, Eq. (3)), which considers thermal gradients. Thus, these preliminary results indicate that using the regular J integral, Eq. (2), for cracks developing in thermally expanded UO_2 fuel pellets is sufficient to calculate stress intensity factors. Also Figure 8 shows that the J and J^* integral computation were independent of contour shape and size (see Figure 5), indicating integration path independence, as would be expected.

2.2 Fuel oxidation model coupled to cracked fuel solid mechanics

The coupling of the solid mechanics model to the fuel oxidation model in 2D is achieved by using the COMSOL® ALE physics module. Figure 9 shows the surfaces which are defined for 'prescribed mesh displacement' by applying the dependent displacement variables u (x coordinate displacement)

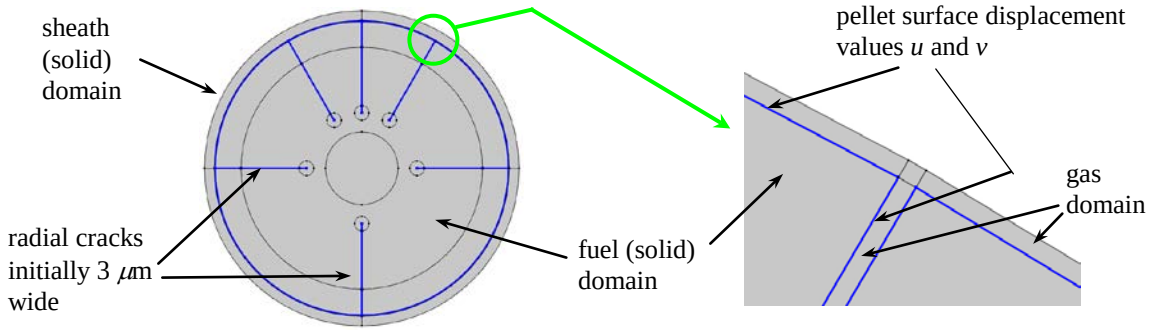

Figure 9 Solid mechanics surfaces indicated in blue for moving the mesh in the fuel cracks and fuel-to-sheath gap outer surfaces using ALE.

and v (y coordinate displacement). In this manner the mesh belonging to the gas domains in the fuel cracks deform and follow the boundaries of the cracked fuel pellets. The six cracks in Figure 9 are full length, initially 3 μm wide, open cracks. Fuel plasticity is not considered here. Quadratic shape functions were applied in all physics and quadrilateral mesh elements were used. The fuel oxidation was allowed to occur at common interfaces between the fuel and gas domains in all six fuel cracks. The time dependent fully coupled model was solved for two weeks of simulated heating and the computation time was about 48 hours. Figure 10 provides the model results for: (a) the temperature distribution, (b) the oxygen stoichiometric deviation distribution and (c) the von Mises stress distribution. The hydrogen mole fraction distribution (q in Eq. (6)) in the fuel cracks and in the fuel-to-sheath gap is not shown here since it is too slender to present as a 2D plot but it would show a minimal value at the sheath breach area and an increasing value (in hydrogen) in the fuel cracks and fuel-to-sheath gap as the distance from the sheath breach is increased. The maximum crack opening expansion was about 100 μm (bottom 6 o'clock crack in Figure 10). The deviation from stoichiometry in the model is highest near the centre of the fuel, x = 0.088, where it is hottest and lowest at the fuel periphery where it is coolest, remembering that crack widths can affect the extent of fuel oxidation [5]. The model results show that the solid mechanics model with the thermally expanded fuel cracks can be coupled with the fuel oxidation model. A similar model would be quite useful in simulating in-reactor high powered defective fuel elements in normal and accident conditions, where crack number and geometry can change.

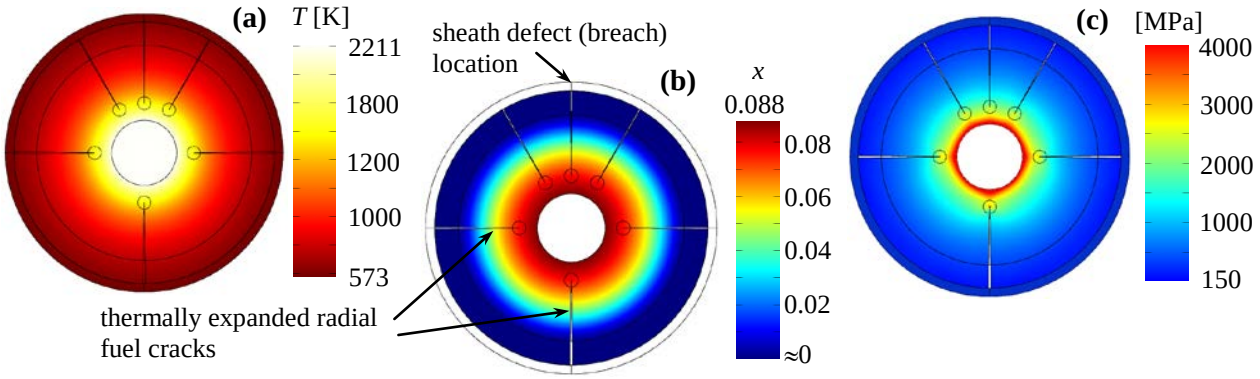

Figure 10 Coupled solid mechanics and fuel oxidation model results that include: (a) temperature distribution, (b) oxygen stoichiometric deviation and (c) von Mises stress distribution after two weeks of simulated heating.

3. Discussion and conclusions

The result of a plane strain steady state solid mechanics model, where stress intensity factors were computed in a pellet surface flaw tip that develops into a fuel crack, showed that crack tip stress intensity factors decrease in magnitude when a plastic fuel core is considered in an out-reactor fuel pellet with inner annulus, compared to a purely elastic fuel case. This is because fuel core plasticity reduces the overall thermal stress in the fuel. With one modelled pre-set radial fuel crack and one developing fuel crack, the computed K_I values were substantially higher than analytical or measured fracture toughness K_{Ic} values of sintered UO_2, which as a result is predicted to cause further fuel cracking and a reduction is K_I values around crack tips. Using a J^* integral that considers thermal

stresses did not produce significantly different K_I results than using the regular J integral in the current study. Computing the J and J^* integrals on difference contour shapes and sizes produced similar results, indicating integration path independence.

It was shown that coupling the solid mechanics model (with thermally expanded fuel cracks) with the time dependent fuel oxidation model can be achieved. The oxidation that was computed in the defected fuel, after two weeks of fuel element heating (which simulates exposure of the fuel to light water at coolant pressures and temperatures) caused a maximum oxygen stoichiometric deviation equal to $x = 0.088$. This result though is expected to be an over estimation of the true oxidation extent [5] since the sheath defect in the 2D r-θ model is longer than in reality. A full sized 3D model makes a more accurate prediction [5].

The effect of this level of oxidation in out-reactor UO_2 fuel is not predicted to substantially change the fuel temperature distribution, and hence the fuel crack geometry. Nevertheless this 2D r-θ coupled model can be modified to represent an in-reactor high powered defective fuel element (during normal and accident conditions), where crack geometry can change substantially due to changes in fuel temperature, which is induced by fuel oxidation.

4. References

[1] B.J Lewis, F.C. Iglesias, D.S. Cox and E. Gheorghiu, "A model for fission gas release and fuel oxidation behaviour for defected UO_2 fuel elements", *Nuclear Technology*, Vol. 92, 1990, pp. 353-362.

[2] K. Une, M. Imamura., M. Amaya and Y. Korei, "Fuel oxidation and irradiation behaviours of defective BWR fuel rods", *J. Nuclear Materials*, Vol. 223, 1995, pp. 40-50.

[3] B.J. Lewis, W.T. Thompson, F. Akbari, D.M. Thompson, C. Thurgood and J. Higgs, "Thermodynamic and kinetic modelling of the fuel oxidation behaviour in operating defective fuel", *J. Nuclear Materials*, Vol. 328, 2004, pp. 180-196.

[4] J.D. Higgs, B.J. Lewis, W.T. Thompson and Z. He, "A conceptual model for the fuel oxidation of defective fuel", *J. Nuclear Materials*, Vol. 366, 2007, pp. 99-128.

[5] A. Quastel, C.M. Thiriet, E.C. Corcoran, B.J. Lewis and F. Abbasian, "Modeling of fuel oxidation with fuel crack and fuel-to-sheath gap dimension dependence applied to an out-reactor instrumented defected fuel experiment", Transactions Division II, SMiRT-22 Conference, San-Francisco, California, USA, 2013 August 18-23.

[6] A.F. Bower, Applied Mechanics of Solids, CRC Press Taylor and Francis Group, Boca Raton, Florida, USA, 2010.

[7] Nonlinear Structural Materials Module User's Guide, COMSOL Multiphysics Version 4.3b, May 2013.

[8] SCDAP/RELAP5 Development Team, Mode3.2 Code Manual, Volume IV: MATPRO, A library of materials properties for light water reactor accident analysis, Idaho National Engineering and Environmental Laboratory, Idaho, 1997.

[9] D.R. Olander, Fundamental aspects of nuclear reactor fuel elements, University of California, Technical Information Center, Energy Research and Development Administration, US Department of Energy, Prepared for Publishing by HP, reprint from the University of

Michigan Libraries Collection, 1976.

[10] D.G. Martin, "The thermal expansion of solid UO_2 and (U, Pu) mixed oxides - A review and recommendations", *J. of Nuclear Materials*, Vol. 152, 1988, pp. 94-101.

[11] E.B. Schwenk, K.R. Wheeler, G.D. Shearer and R.T. Webster, *J. Nuclear Materials*, Vol. 78, 1978, pp. 129-131.

[12] J.E. Talia and F. Povolo, "Tensile properties of Zircaloy-4", *J. Nuclear Materials* Vol. 67, 1977, pp. 198-206.

[13] D.O. Hobson, "The collapse behavior of Zircaloy fuel cladding", Metals and Ceramics Division, Oak Ridge National Laboratory, Oak Ridge Tennessee 37830 , DOE OSTI 729092, March 1976.

[14] T. Tachibana, H. Furuya and M. Koizumi, "Dependence on strain rate and temperature shown by yield stress of uranium dioxide", *J. of Nuclear Science and Technology*, Vol. 16(9), 1976, pp. 497-502.

[15] M. Oguma, "Cracking and relocation behaviour of nuclear fuel pellets during rise to power", *Nuclear Engineering and Design*, Vol 76, 1983, pp. 35-45.

[16] O.C. Zienkiewicz and R.L Taylor, The finite element method 6th Ed., McGraw-Hill, 2005

[17] J.R. Rice, "A path independent integral and approximate analysis of strain by notches and cracks", *J. Applied Mechanics*, Vol. 35, 1968, pp. 379-386.

[18] T.L. Anderson, Fracture Mechanics Fundamentals and Applications, 3rd Ed., Taylor and Francis Group, 2005.

[19] W.K. Wilson and I.W. Yu, "The use of the *J*-integral in thermal stress crack problems", *International Journal of Fracture*, Vol. 15, No. 4, August 1979, pp. 377-387.

[20] S. Aoki, K. Kishimoto and M. Sakata, "Elastic-plastic analysis of crack in thermally-loaded structures", *Engineering Fracture Mechanics* Vol. 16(3), 1982, pp. 405-413.

[21] M. Janssen, J. Zuidema and R.J.H. Wanhill, Fracture Mechanics, VSSD 2nd Ed., Netherlands, 2006.

[22] T.R.G. Kutty, K.N. Chandrasekharan, J.P. Panakkal and J.K. Ghosh, "Fracture toughness and fracture surface energy of sintered uranium dioxide fuel pellets", *J. Materials Science Letters*, Vol. 6, 1987, pp. 260-262.

[23] C. Bernaudat, "Mechanical behaviour modelling of fractured nuclear fuel pellets", *Nuclear Engineering and Design*, Vol. 156, 1995, pp. 373-381.

[24] K. Shaheen, A.D. Quastel, J.S. Bell, B.J. Lewis, W.T. Thompson and E.C. Corcoran, "Modelling CANDU fuel element and bundle behaviour for in-reactor and out-reactor performance of intact and defective fuel", 11th International Conference on CANDU Fuel, Niagara Falls Ontario, Canada, October 17-20 2010.

[25] A.M. Ross and R.L. Stoute, "Heat transfer coefficient between UO_2 and Zircaloy-2", Atomic Energy Canada Ltd., AECL-1552, 1962.